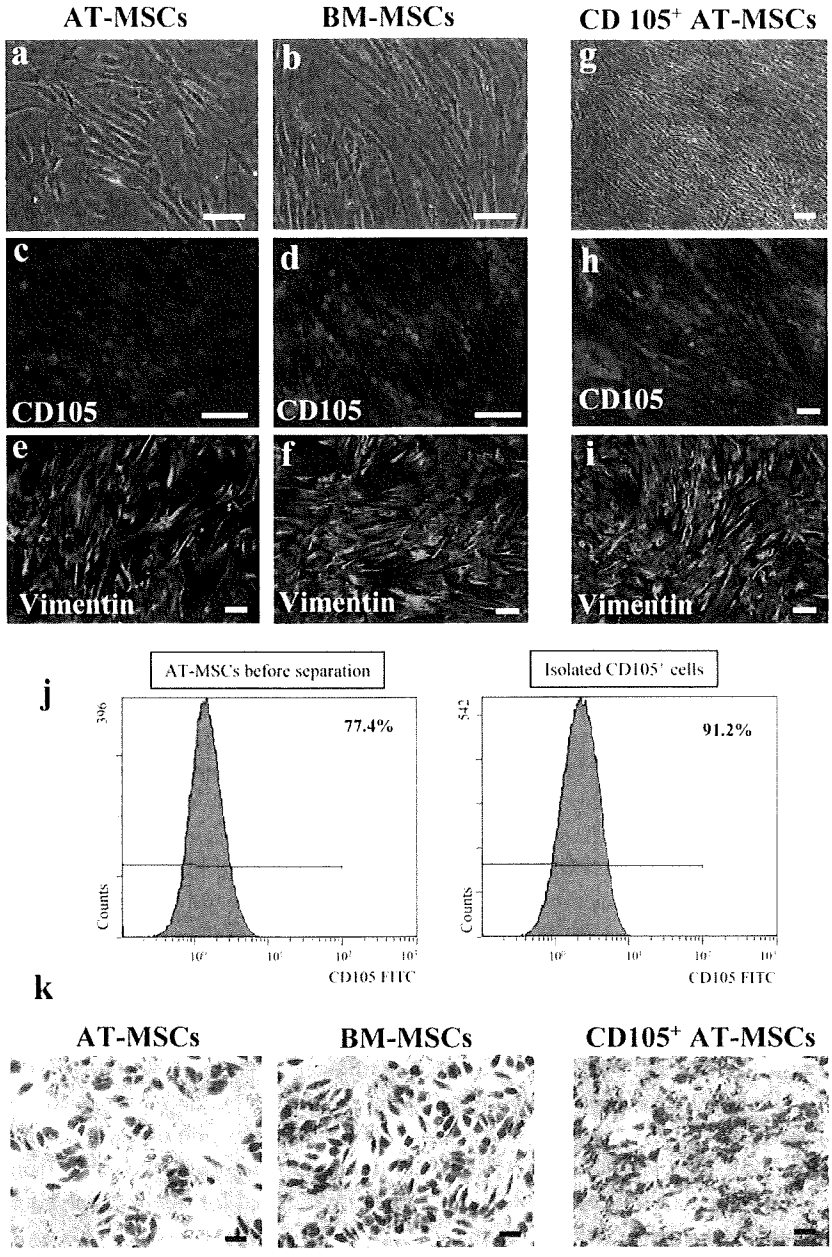

Fig. 2. Morphology of AT-MSCs (a) and BM-MSCs (b). Both types of cells were stained for CD105 (rhodamine, red) and vimentin (FITC, green); AT-MSCs (c and e) and BM-MSCs (d and f). MACS sorting resulted in achievement of a homogeneous population (g). $CD105^+$ AT-MSCs were stained for CD105 (h) and vimentin (i). Before and after MACS sorting cells were analyzed by flow cytometry for CD105 (j). BM-MSCs, AT-MSCs unfractionated, and $CD105^+$ AT-MSCs were cultured for 3 weeks in an adipogenic induction medium and analyzed by Oil red O staining (k). Scale bars represent 50μm.

hepatocyte-specific markers and transcription factor similar to human hepatocytes.

Immunostaining and Western Blot Confirmation of Hepatic Differentiation. In the next experiments, we examined whether, $CD105^+$ AT-MSCs expressed hepatocyte-specific proteins after hepatic induction. Markers such as ALB, TTR, CYP3A4, and CK-18 were positively stained using immunofluorostaining. We detected double-positive cells for ALB/CYP3A4, CK-18/TTR (Fig. 5A), and ALB/TTR (data not shown) at day 40. Undifferentiated cells were not stained on all these four markers (data not shown). To further confirm efficient hepatic induction, we checked the protein expression of the hepatocyte-specific enzymes CYP1A1, CYP3A4, CYP2C9 and NAPDH P-450 reductase by Western blot analysis (Fig. 5B). A clear band for all four proteins was detected in $CD105^+$ AT-MSC-derived hepatocyte-like cells (Fig. 5B, lane 2). Undifferentiated $CD105^+$ AT-MSCs (Fig. 5B, lane 1) express a low, detectable level of CYP1A1 as well, as had been observed in RT-PCR analysis (data not shown).

Functional Characterization of AT-MSC-Derived Hepatocytes. Afterwards, we examined whether hepatocytes derived from $CD105^+$ AT-MSCs are functionally

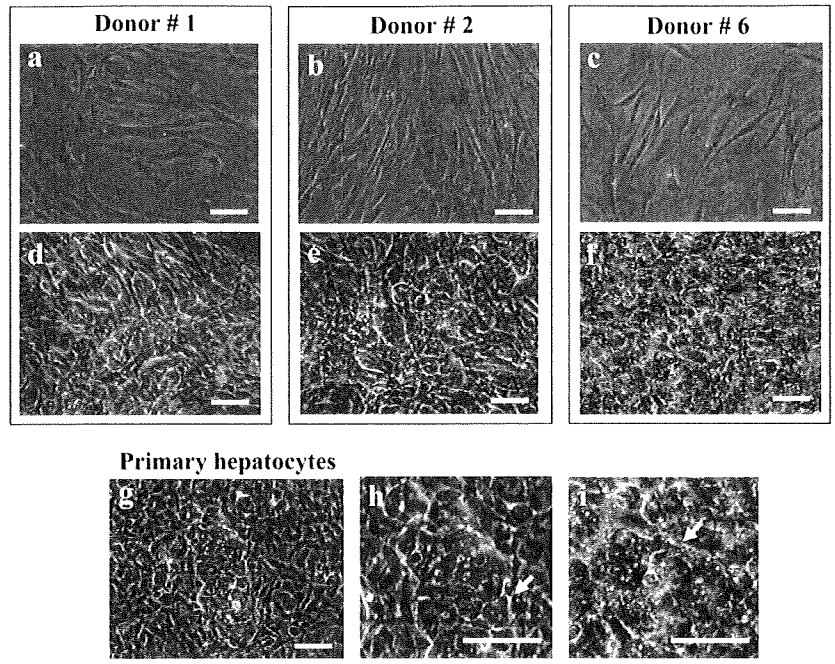

Fig. 3. Undifferentiated CD105$^+$ AT-MSCs from 3 donors (a,b,c) and the same cells after 40 days of hepatic induction (d,e,f). Photograph (i) represents higher magnification of (f). The morphology of CD105$^+$ AT-MSC-derived hepatocyte-like cells represents many similarities with the primary human hepatocytes (g). Photograph (h) represents higher magnification of (g). Arrows indicate bile canaliculi structures. Scale bars represent 50μm.

competent. After 2 weeks of hepatic induction, almost 20% of the cells could incorporate LDL, and, during maturation (40 days), almost all of the induced cells turned out to be competent for LDL uptake (Fig. 5C). At 35 days, CD105$^+$ AT-MSCs were analyzed for their glycogen-storage ability by PAS staining. As shown in Fig. 5D, almost all CD105$^+$ AT-MSC-derived hepatocytes were strongly positive for PAS staining, while undifferentiated CD105$^+$ AT-MSCs were weakly positive. Moreover, we examined their abilities to produce albumin and detoxify ammonia. Our analyses indicate that AT-MSC-de-

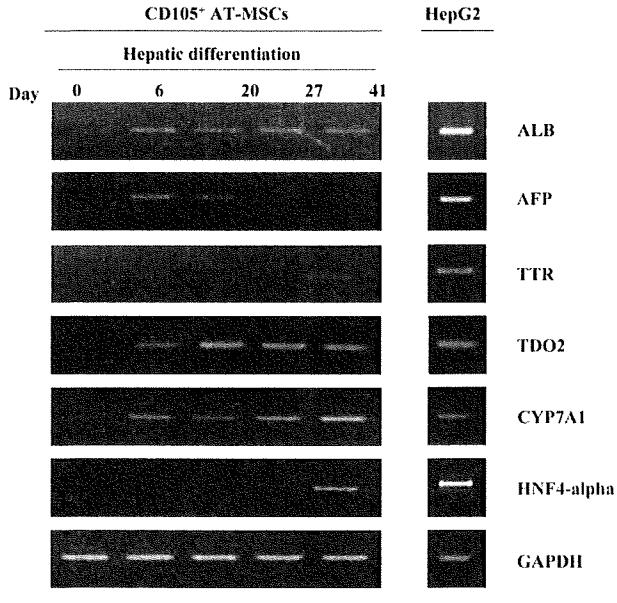

Fig. 4. RT-PCR of a temporal gene expression pattern of hepatocyte-specific markers during hepatic differentiation of CD105$^+$ AT-MSCs. RNA was isolated from undifferentiated CD105$^+$ AT-MSCs (day 0) and from CD105$^+$ AT-MSCs during hepatic induction at days 6, 20, 27, and 41.

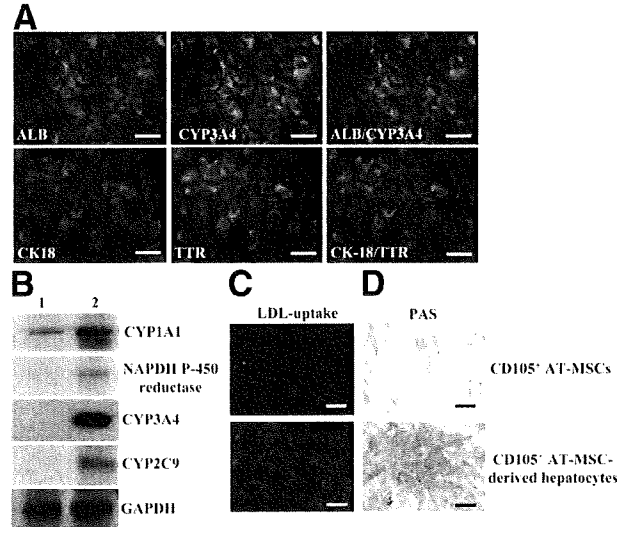

Fig. 5. Immunofluorostaining analysis of hepatocyte-specific markers in differentiated CD105$^+$ AT-MSCs (A). At day 40, cells were fixed and stained with monoclonal antibodies against sequentially ALB, CK-18 (red), CYP3A4, and TTR (green). Western blot analysis indicated that CYP1A1 (58.2kDa), NADPH P-450 reductase (76.5 kDa), CYP2C9 (56 kDa) and CYP3A4 (57 kDa), were actively synthesized in CD105$^+$ AT-MSC-derived hepatocytes (lane 2), GAPDH was used as an internal control (35 kDa) (B) (lane 1). CD105$^+$ AT-MSCs-derived hepatocyte-like cells were analyzed for ability of LDL-uptake (C) and glycogen storage ability, using PAS (periodic acid Schiff) staining (D). Scale bars represent 50μm.

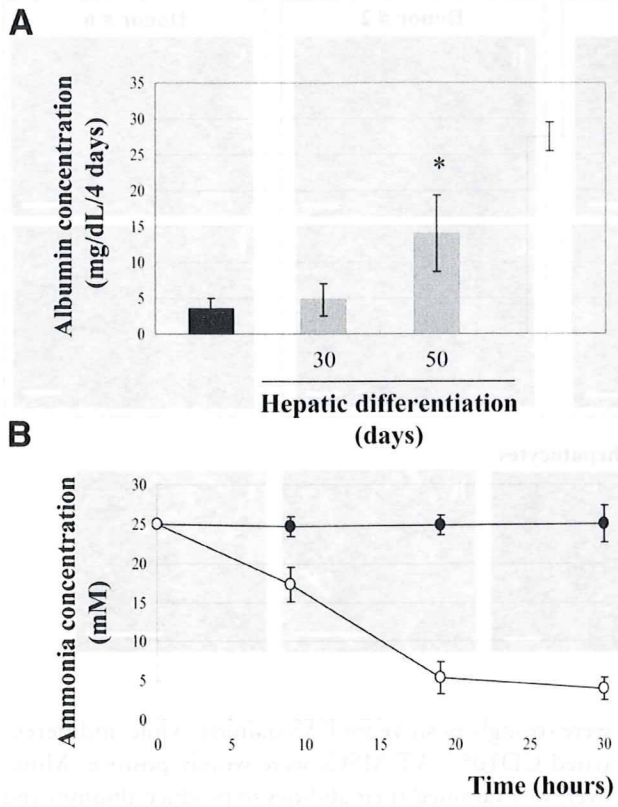

Fig. 6. (A) Albumin production of CD105$^+$ AT-MSCs (shaded square) during hepatic differentiation (at day 30 and 50), undifferentiated CD105$^+$ AT-MSCs (filled square), and primary human hepatocytes (open square). Graph (B) shows ammonia detoxification by CD105$^+$ AT-MSC-derived hepatocytes (open circle). Undifferentiated CD105$^+$ AT-MSCs (filled circle) did not reveal the ability to clear ammonia from the culture medium. Data are reported as the mean ± SD and were analyzed by the Student t test, n = 3. * $P < 0.05$).

rived hepatocytes have the capacity to secrete albumin (Fig. 6A) and clear ammonia from culture media (Fig. 6B). In addition, although data are not shown, we detected the CYP3A4 activity of CD105$^+$ AT-MSC-derived hepatocytes. These data taken together indicate that CD105$^+$ AT-MSC-derived hepatocyte-like cells exhibit liver-specific functions similar to normal matured human hepatocytes.

Transplantation of CD105$^+$ AT-MSC-Derived Hepatocytes into Mice with CCl_4 Injury. Finally, we addressed our ultimate goal, namely, examining whether our generated hepatocytes were therapeutically applicable. We transplanted 5 × 10^5 CD105$^+$ AT-MSC-derived hepatocytes into CCl_4-injured mouse. Hematoxylin-eosin staining showed damage to the liver after a CCl_4 injection (Fig. 7a-c). Twenty-four hours after transplantation of undifferentiated CD105$^+$ AT-MSCs and CD105$^+$ AT-MSC-derived hepatocytes liver sections were examined by human specific albumin immunostaining (Fig. 7d-f) and revealed that CD105$^+$ AT-MSC-derived hepatocytes were incorporated into host livers. In those mice, some liver functions were improved such as ammonia concentration level, as well as a marker of the damaged liver-glutamic-pyruvic aminotransferase (GPT) (data not shown) level in the peripheral blood. Some human albumin-positive cells have been found in liver sections after implantation of undifferentiated CD105$^+$ AT-MSCs; however, these cells exhibited no typical hepatocyte morphology (Fig. 7b,e). In summary, our AT-MSC-derived hepatocyte-like cells are applicable for transplantation.

Discussion

Transplantation of hepatocytes might become easier, efficient, and safer than whole organ transplantation to cure patients suffering from end-stage liver dysfunction. The

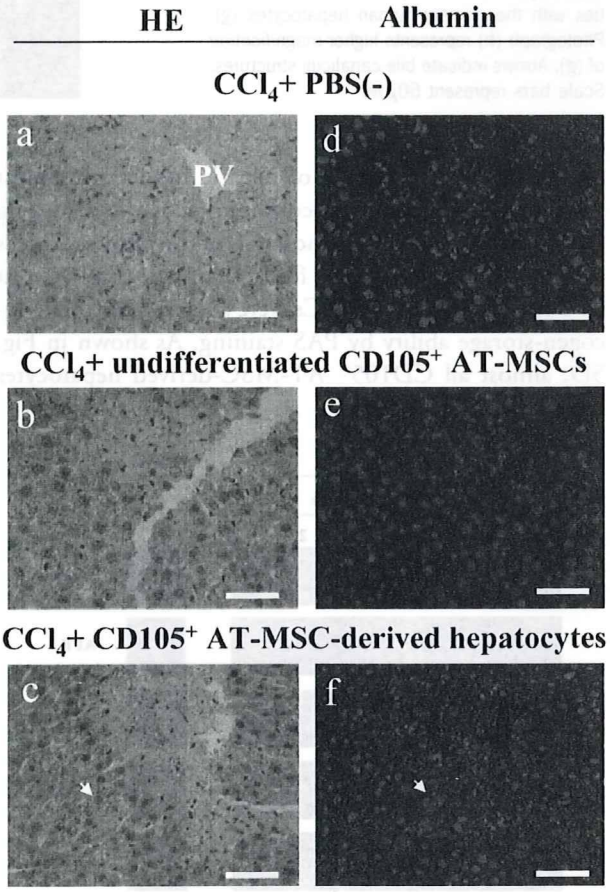

Fig. 7. Transplantation of CD105$^+$ AT-MSC-derived hepatocytes into mice with CCl_4 injury. Histological sections were stained with anti-human specific albumin antibodies. Hematoxylin Eosin (HE) staining of a liver section from CCl_4-treated mice administered with PBS (−) (n = 3) (a), HE staining of a liver section from CCl_4-treated mice 1 day after transplantation of undifferentiated CD105$^-$ AT-MSCs (n = 3) (b) and CD105$^+$ AT-MSC-derived hepatocytes (n = 3) (c). Panels (d), (e), (f) represent the subsequent human ALB immunostaining of serial sections of (a), (b), (c). The arrows point to the stained cells integrated with hepatic areas in clusters. PV, portal vein. Scale bars represent 50μm.

maintenance of hepatocyte function *in vitro* is difficult if not nearly impossible. The generation of stem cell-derived hepatocytes holds considerable promise for future clinical applications. The hepatogenic potential of MSCs from different sources has been previously described.[7-10] There have been two reports so far indicating the endoderm differentiation capacity of AT-MSCs (insulin-, somatostatin-, and glucagon-expressing cells[9,10] as well as ALB- and AFP-expressing hepatocyte-like cells with the ability to synthesize urea and uptake LDL[33]); however, the second reported system includes the use of DMSO, which has been shown to maintain hepatic morphology. In contrast, our system simulates *in vivo* endoderm development of the liver, as previously reported.[2,3] Concerning the donation procedure, isolation ratio, and minimal decline in donor health, we postulate that AT-MSCs represent an attractive tool for studies on stem cell therapy for the liver. MSCs from a predominant source, such as bone marrow, reveal a lower proliferation capacity and frequency than AT-MSCs,[28] and their frequency is influenced by age, gender, the presence of osteoporosis, and prior exposure to high-dose chemotherapy or radiation. Importantly, from 200ml of lipoaspirate, it is possible to obtain approximately 40-fold more stem cells than from 40 ml of marrow.[21] Even though adipose tissue provides a more heterogeneous population of stem cells, the potential number of AT-MSCs is sufficiently large to allow the selection/sorting of the multipotential fraction of AT-MSCs. The $CD105^+$ fraction from BM-MSCs has been reported to have more homogeneity and a greater ability to form CFU-Fs.[37-39] In order to select multipotent AT-MSCs, some scientists have used other isolation procedures[41]; we selected a $CD105^+$ fraction using magnetic beads. Insofar as the $CD105^+$ fraction of BM-MSCs is age-resistant,[39] sorting might be very useful because many patients with liver failure or hepatocarcinoma are elderly. Large amounts of fat are discarded during liposuction, and, in the future, this valuable resource could be used for the isolation of AT-MSCs, which might then be stored in each patient's cell bank.

We have demonstrated the ability of $CD105^+$ AT-MSCs to undergo hepatic differentiation, resulting in the achievement of functional and transplantable hepatocytes (60%-85%). Unfractionated AT-MSCs revealed hepatogenic potentiality as well; however, the ratio of differentiation was lower (20%-60%). The hepatogenic potentiality of AT-MSCs was confirmed by the detection of hepatic-specific markers and biochemical functions. The major protein produced by the hepatocytes, ALB, was synthesized and secreted into a medium at days 30 and 50 (subsequently: 5 and 14 mg/dl/4days/10^6 cells). The expression and activity of the microsome CYP enzymes involved in drug, xenobiotic metabolism, and sterol and bile acid synthesis indicates hepatocyte specificity. Generated from $CD105^+$ AT-MSCs, hepatocytes express CYP7A1, CYP1A1, CYP2C9, CYP3A4, and NADPH-cytochrome P450 reductase. Therefore, these findings suggest that there might be value in *in vitro* preclinical drug investigations.

We then implanted *in vitro* generated hepatocytes into CCl_4-injured nude mice and observed direct incorporation into the liver, which was confirmed by human albumin immunostaining. Our induction system does not require co-culturing, thus undesired cell-cell interactions are reduced; nevertheless, further studies examining the *in vivo* mechanism of homing, engraftment, and liver regeneration need to be performed in order to eliminate post-transplantation complications. We observed that some *in vivo* functions, such as the serum ammonia level and GPT, decrease after transplantation of undifferentiated AT-MSCs (data not shown) as well. These findings indicate the possibility of *in vivo* differentiation of AT-MSCs caused by a regeneration microenvironment. The subsequent interaction of transplanted undifferentiated MSCs with liver parenchyma cells also needs to be evaluated in the context of the promotion of fibrosis,[42] cancer, or liver dysfunction. Another topic of interest deserving evaluation is the correlation between factors such as donor age, cancer record, and the differentiation potentiality of stem cells. It should be emphasized that three independent donor-derived $CD105^+$ AT-MSCs showed similar hepatic differentiation ability. In the context of clinical application, the usage of AT-MSCs, which can be obtained from a patient's own tissue in contrast to highly potent ES cells, would eliminate many obstacles such as ethical issues, rejection and the risk of teratoma and tumor formation.

In summary, we have presented *in vitro* production of functional and transplantable hepatocytes from adipose tissue-derived mesenchymal stem cells. Our findings, combined with the development of tissue engineering technologies, may support stem cell-based therapy for liver injuries and for the establishment of a bioartificial liver.

Acknowledgment: We would like to thank Dr. Satoshi Suzuki (Human and Animal Bridging Research Organization), Ms. Nachi Namatame, Dr. Kazunori Aoki, Dr. Akihiro Kobayashi, Ms. Ayako Inoue, Ms. Maho Kodama and Ms. Shinobu Ueda (National Cancer Center Research Institute) for their valuable advice and assistance.

References

1. Lavon N, Benvenisty N. Study of hepatocyte differentiation using embryonic stem cells. J Cell Biochem 2005;96:1193-1202.
2. Teratani T, Yamamoto H, Aoyagi K, Sasaki H, Asari A, Quinn Q, et al. Direct hepatic fate specification from mouse embryonic stem cells. HEPATOLOGY 2005;41:836-846.

3. Yamamoto Y, Teratani T, Yamamoto H, Quinn G, Murata S, Ikeda R, et al. Recapitulation of in vivo gene expression during hepatic differentiation from embryonic stem cells. HEPATOLOGY 2005;42:558-567.
4. Yamamoto H, Quinn Q, Asari A, Yamanokuchi H, Teratani T, Terada M, et al. Differentiation of embryonic stem cells into hepatocytes: biological functions and therapeutic application. HEPATOLOGY 2003;37:983-993.
5. Petersen BE, Bowen WC, Patrene KD, Mars WM, Sullivan AK, Murase N, et al. Bone marrow as a potential source of hepatic oval cells. Science 1999; 284:1168-1170.
6. Theise ND, Badve S, Saxena R, Henegariu O, Sell S, Crawford JM, et al. Derivation of hepatocytes from bone marrow cells in mice after radiation-induced myeloablation. HEPATOLOGY 2000;31:235-240.
7. Schwartz RE, Reyes M, Koodie L, Jiang Y, Blackstad M, Lund T, et al. Multipotent adult progenitor cells from bone marrow differentiate into functional hepatocyte-like cells. J Clin Invest 2002;109:1291-1302.
8. Sato Y, Araki H, Kato J, Nakamura K, Kawano Y, Kobune M, et al. Human mesenchymal stem cells xenografted directly to rat liver are differentiated into human hepatocytes without fusion. Blood 2005;106:756-763.
9. Ong SY, Dai H, Leong KW. Inducing hepatic differentiation of human mesenchymal stem cells in pellet culture. Biomaterials 2006;27:4087-4097.
10. Hong SH, Gang EJ, Jeong JA, Ahn C, Hwang SH, Yang IH, et al. In vitro differentiation of human umbilical cord blood-derived mesenchymal stem cells into hepatocyte-like cells. Biochem Biophys Res Commun 2005;330: 1153-1161.
11. Pittenger MF, Mackay AM, Beck SC, Jaiswal RK, Douglas R, Mosca JD, et al. Multilineage potential of adult human mesenchymal stem cells. Science 1999;284:143-147.
12. Zuk PA, Zhu M, Mizuno H, Huang J, Futrell JW, Katz AJ, et al. Multilineage cells from human adipose tissue: implications for cell-based therapies. Tissue Eng 2001;7:211-228.
13. Zuk PA, Zhu M, Ashjian P, De Ugarte DA, Huang JI, Mizuno H, et al. Human adipose tissue is a source of multipotent stem cells. Mol Biol Cell 2002;13:4279-4295.
14. Shih DT, Lee DC, Chen SC, Tsai RY, Huang CT, Tsai CC, et al. Isolation and characterization of neurogenic mesenchymal stem cells in human scalp tissue. Stem Cells 2005;7:1012-1020.
15. In't Anker PS, Scherjon SA, Kleijburg-van der Keur C, de Groot-Swings GM, Claas FH, Fibbe WE, et al. Isolation of mesenchymal stem cells of fetal or maternal origin from human placenta. Stem Cells 2004;22:1338-1345.
16. Bieback K, Kern S, Kluter H, Eichler H. Critical parameters for the isolation of mesenchymal stem cells from umbilical cord blood. Stem Cells 2004;22:625-634.
17. Campagnoli C, Roberts IA, Kumar S, Bennett PR, Bellantuono I, Fisk NM. Identification of mesenchymal stem/progenitor cells in human first-trimester fetal blood, liver, and bone marrow. Blood 2001;98:2396-2402.
18. Ferrari G, Cusella-DeAngelis G, Coletta M, Paolucci E, Stornaiuolo A, Cossu G, et al. Muscle regeneration by bone marrow-derived myogenic progenitors. Science 1998;279:1528-1530.
19. Sanchez-Ramos J, Song S, Cardozo-Pelaez F, Hazzi C, Stedeford T, Willing A, et al. Adult bone marrow stromal cells differentiate into neural cells in vitro. Exp Neurol 2000;164:247-256.
20. De Ugarte DA, Morizono K, Elbarbary A, Alfonso ZC, Zuk PA, Zhu M, et al. Comparison of multi-lineage cells from human adipose tissue and bone marrow. Cells Tissues Organs 2003;174:101-109.
21. Strem BM, Hicok KC, Zhu M, Wulur I, Alfonso ZC, Schreiber RE, et al. Multipotential differentiation of adipose tissue-derived stem cells. Keio J Med 2005;54:132-141.
22. Katz AJ, Tholpady A, Tholpady SS, Shang H, Ogle RC. Cell surface and transcriptional characterization of human adipose-derived adherent stromal (hADAS) cells. Stem Cells 2005;23:412-423.
23. Brzoska M, Geiger H, Gauer S, Baer P. Epithelial differentiation of human adipose tissue-derived adult stem cells. Biochem Bioph Res Co 2005;330: 142-150.
24. Guilak F, Lott KE, Awad HA, Cao Q, Hicok KC, Fermor B, et al. Clonal analysis of the differentiation potential of human adipocyte-derived adult stem cells. J Cell Physiol 2006;206:229-237.
25. Lee RH, Kim B, Choi I, Kim H, Choi HS, Suh K, et al. Characterization and expression analysis of mesenchymal stem cells from human bone marrow and adipose tissue. Cell Physiol Biochem 2004;14:311-324.
26. Wagner W, Wein F, Seckinger A, Frankhauser M, Wirkner U, Krause U, et al. Comparative characteristics of mesenchymal stem cells from human bone marrow, adipose tissue, and umbilical cord blood. Exp Hematol 2005;33:1402-1416.
27. Gronthos S, Franklin DM, Leddy HA, Robey PG, Storms RW, Gimble JM. Surface protein characterization of human adipose tissue-derived stromal cells. J Cell Physiol 2001;189:54-63.
28. Kern S, Eichler H, Stoeve J, Kluter H, Bieback K. Comparative analysis of mesenchymal stem cells from bone marrow, umbilical cord blood or adipose tissue. Stem Cells 2006;24:1294-1301.
29. Dicker A, Le Blanc K, Astrom G, Van Harmelen V, Gotherstrom C, Blomqvist L, et al. Functional studies of mesenchymal stem cells derived from adult human adipose tissue. Exp Cell Res 2005;308:283-290.
30. Im GI, Shin YW, Lee KB. Do adipose tissue–derived mesenchymal stem cells have the same osteogenic and chondrogenic potential as bone marrow-derived cells? Osteoarthr Cartilage 2005;13:845-853.
31. Safford KM, Hicok KC, Safford SD, Halvorsen YD, Wilkison WO, Gimble JM, et al. Neurogenic differentiation of murine and human adipose-derived stromal cells. Biochem Biophys Res Commun 2002;294:371-379.
32. Cao Y, Sun Z, Liao L, Meng Y, Han Q, Zhao RC. Human adipose tissue-derived stem cells differentiate into endothelial cells in vitro and improve postnatal neovascularization in vivo. Biochem Biophys Res Commun 2005;332:370-379.
33. Seo MJ, Suh SY, Bae YC, Jung JS. Differentiation of human adipose stromal cells into hepatic lineage in vitro and in vivo. Biochem Biophys Res Commun 2005;328:258-264.
34. Boquest AC, Shahdadfar A, Fronsdal K, Sigurjonsson O, Tunheim SH, Collas P, et al. Isolation and transcription profiling of purified uncultured human stromal stem cells: alteration of gene expression after in vitro cell culture. Mol Biol Cell 2005;16:1131-1141.
35. Haynesworth SE, Baber MA, Caplan AI. Cell surface antigens on human marrow-derived mesenchymal stem cells are detected by monoclonal antibodies. Bone 1992;13:69-80.
36. Liu PG, Zhou DB, Shen T. Identification of human bone marrow mesenchymal stem cells: preparation and utilization of two monoclonal antibodies against SH2, SH3. (in Chinese) Zhongguo Shi Yan Xue Ye Xue Za Zhi 2005;13:656-659.
37. Aslan H, Zilberman Y, Kandel A, Liebergall M, Oskouian RJ, Gazit D, et al. Osteogenic differentiation of noncultured immunoisolated bone marrow-derived CD105$^+$ cells. Stem Cells 2006;24:1728-1737.
38. Majumdar MK, Banks V, Peluso DP, Morris EA. Isolation, characterization, and chondrogenic potential of human bone marrow-derived multipotential stromal cells. J Cell Physiol 2000;185:98-106.
39. Roura S, Farre J, Soler-Botija C, Llach A, Hove-Madsen L, Cairo JJ, et al. Effect of aging on the pluripotent capacity of human CD105$^+$ mesenchymal stem cells. Eur J Heart Fail 2006;8:555-563.
40. Timper K, Seboek D, Eberhardt M, Linscheid P, Christ-Crain M, Keller U, et al. Human adipose tissue-derived mesenchymal stem cells differentiate into insulin, somatostatin, and glucagon expressing cells. Biochem Biophys Res Commun 2006;341:1135-1140.
41. Rodriguez AM, Elabd C, Delteil F, Astier J, Vernochet C, Saint-Marc P, et al. Adipocyte differentiation of multipotent cells established from human adipose tissue. Biochem Biophys Res Commun 2004;315:255-263.
42. Russo FP, Alison MR, Bigger BW, Amofah E, Florou A, Amin F, et al. The bone marrow functionally contributes to liver fibrosis. Gastroenterology 2006;130:1807-1821.

the FEBS Journal

A comparative analysis of the transcriptome and signal pathways in hepatic differentiation of human adipose mesenchymal stem cells

Yusuke Yamamoto[1,2,*], Agnieszka Banas[1,*], Shigenori Murata[3], Madoka Ishikawa[3], Chun R. Lim[3], Takumi Teratani[1], Izuho Hatada[4], Kenichi Matsubara[3], Takashi Kato[2] and Takahiro Ochiya[1,2]

1 Section for Studies on Metastasis, National Cancer Center Research Institute, Tokyo, Japan
2 Graduate School of Science and Engineering, Waseda University, Tokyo, Japan
3 DNA Chip Research Inc., Yokohama, Japan
4 Laboratory of Genome Science, Biosignal Genome Resource Center, Department of Molecular and Cellular Biology, Gunma University, Maebashi, Japan

Keywords
adipose tissue; gene ontology; hepatocyte differentiation; mesenchymal stem cell; microarray

Correspondence
T. Ochiya, Section for Studies on Metastasis, National Cancer Center Research Institute, 1-1 Tsukiji 5-chome, Chuo-ku, Tokyo 104-0045, Japan
Fax: +81 3 3541 2685
Tel: +81 3 3542 2511(ext 4452)
E-mail: tochiya@ncc.go.jp

*These authors contributed equally to this work

(Received 30 October 2007, revised 26 December 2007, accepted 10 January 2008)

doi:10.1111/j.1742-4658.2008.06287.x

The specific features of the plasticity of adult stem cells are largely unknown. Recently, we demonstrated the hepatic differentiation of human adipose tissue-derived mesenchymal stem cells (AT-MSCs). To identify the genes responsible for hepatic differentiation, we examined the gene expression profiles of AT-MSC-derived hepatocytes (AT-MSC-Hepa) using several microarray methods. The resulting sets of differentially expressed genes (1639 clones) were comprehensively analyzed to identify the pathways expressed in AT-MSC-Hepa. Clustering analysis revealed a striking similarity of gene clusters between AT-MSC-Hepa and the whole liver, indicating that AT-MSC-Hepa were similar to liver with regard to gene expression. Further analysis showed that enriched categories of genes and signaling pathways such as complementary activation and the blood clotting cascade in the AT-MSC-Hepa were relevant to liver-specific functions. Notably, decreases in Twist and Snail expression indicated that mesenchymal-to-epithelial transition occurred in the differentiation of AT-MSCs into hepatocytes. Our data show a similarity between AT-MSC-Hepa and the liver, suggesting that AT-MSCs are modulated by their environmental conditions, and that AT-MSC-Hepa may be useful in basic studies of liver function as well as in the development of stem cell-based therapy.

Mesenchymal stem cells (MSCs) are the most promising candidates with respect to clinical applications in regenerative medicine. MSCs were first isolated from bone marrow cells by simple plating on plastic dishes [1]. Further studies demonstrated evidence of their presence in adipose tissue [2,3], scalp tissue [4], placenta [5], amniotic fluid and umbilical cord blood [6], as well as in various fetal tissues [7]. Importantly, these stem cells can differentiate *in vitro* into multiple types of cells, including chondrocytes, osteocytes, adipocytes [8], myocytes [9], neurons [10] and hepatocytes, depending on the appropriate stimuli and microenvironment. MSCs are promising candidates for liver regeneration [11,12], because their usage might overcome obstacles such as ethical concerns and the risks of rejection in cell transplantation therapy.

Abbreviations
ABC transporter, ATP binding cassette transporter; AT-MSC, adipose tissue-derived mesenchymal stem cells; AT-MSC-Hepa, AT-MSC-derived hepatocytes; CYP, cytochrome P450; EMT, epithelial-to-mesencyhmal transition; ES, embryonic stem; FGF, fibroblast growth factor; GO, gene ontology; HGF, hepatocyte growth factor; HIFC, hepatic induction factor cocktail; HNF, hepatocyte nuclear facor; LDL, low-density lipoprotein; MDR, multi-drug resistance; MET, mesencyhmal-to-epithelial transition; MSCs, Mesenchymal stem cells; OsM, oncostatin M; TDO2, tryptophan 2,3-dioxygenase.

Seo *et al.* were the first to show that human adipose tissue-derived mesenchymal stem cells (AT-MSCs) differentiate into hepatocyte-like cells upon treatment with hepatocyte growth factor (HGF), oncostatin M and dimethyl sulfoxide [13]. These cells expressed albumin and α-fetoprotein during differentiation and demonstrated low-density lipoprotein (LDL) uptake and production of urea. Further studies by Toles-Visconti *et al.* also demonstrated the possibility of generating hepatocyte-like cells from AT-MSCs [14]. Many investigators have since used MSCs to generate functional hepatocytes; however, there are still questions regarding cell fusion and poor functionality, which need to be resolved before clinical use.

Based on a study of embryonic stem (ES) cell transplantation, we have identified a growth factor combination [HGF and fibroblast growth factors 1 and 4 (FGF1 and FGF4)] to induce mouse ES cells to develop into functional hepatocytes. These factors, named HIFC (hepatic induction factor cocktail), showed clearly up-regulated expression in an injured liver [15]. Recently, using a modified hepatic differentiation strategy for mouse ES cells, we have successfully differentiated AT-MSCs to hepatocytes [16]. The cells generated from AT-MSCs were transplantable hepatocyte-like cells with functional and morphological similarities to hepatocytes. AT-MSC-derived hepatocytes (AT-MSC-Hepa) demonstrated several liver-specific markers and functions, such as albumin production, LDL uptake and ammonia detoxification. However, the molecular mechanisms underlying the differentiation of AT-MSC are largely unknown. Our next goal is to clarify the molecular events involved in controlling the plasticity of AT-MSCs that give rise to hepatocytes. In this study, we show that the gene expression pattern of AT-MSC-Hepa is similar to that of adult human hepatocytes and liver by microarray analysis. Moreover, the enriched categories of genes and the signaling pathways in the AT-MSC-Hepa were relevant to liver-specific functions.

Results

Microarray analysis of AT-MSC-Hepa

We previously established the HIFC differentiation system, based on a study of ES cell transplantation into CCl_4-injured mouse liver [15]. The identified hepatic induction factors (a combination of HGF, FGF1 and FGF4) were clearly up-regulated in the injured mouse liver. Using a modified HIFC differentiation system, human AT-MSCs can be differentiated into hepatocytes *in vitro* within approximately 5 weeks [16]. This novel system is reproducible and allows examination of the molecular mechanisms underlying hepatic differentiation from stem cells. For microarray analysis, we confirmed the hepatic differentiation of AT-MSC into hepatocyte-like cells using the original protocol (Fig. 1A). The differentiated cells (AT-MSC-Hepa) had a round epithelial cell-like shape (Fig. 1C), while undifferentiated AT-MSCs showed a fibroblast-like morphology (Fig. 1B). During the transition, contraction of the cytoplasm progressed, and most of the treated cells became quite dense and round with clear nuclei (Fig. 1C). We checked albumin expression by immunochemical staining to examine the cell population of AT-MSC-Hepa for microarray analysis. This analysis showed that the AT-MSC-Hepa cell population was almost totally homogeneous ([16], and data not shown). Furthermore, glycogen storage was also observed in AT-MSC-Hepa by periodic acid-Schiff staining (Fig. 1E), but such staining was only weakly positive in undifferentiated AT-MSCs (Fig. 1D). In order to confirm the hepatic induction of AT-MSCs, we analyzed genes related to hepatic differentiation by microarray analyses performed using total RNA from undifferentiated AT-MSCs, AT-MSC-Hepa, human primary hepatocytes and human liver. The profile for undifferentiated AT-MSCs was compared to that of AT-MSC-Hepa. Of the 25 721 genes analyzed, 1639 showed a significant ≥ 10-fold alteration of the expression level, indicating that the expression levels of these genes were regulated by hepatic induction factors.

Of the 1639 genes with a ≥ 10-fold alteration in expression, 1252 genes were up-regulated (supplementary Table S1), and 387 were down-regulated (supplementary Table S2). Up-regulated genes belonged to families of metabolic enzymes, such as alcohol dehydrogenase, UDP glucuronosyltransferase and serine protease inhibitor, and liver marker genes, such as glucose-6-phosphatase and keratin 8 (supplementary Table S1). Additionally, the gene expression levels of hepatocyte marker genes [albumin, tryptophan 2,3-dioxygenase (TDO2), transthyretin and keratin 18] and liver-specific transcription factors such as FOXA2 [hepatocyte nuclear factor (HNF) 3β] and ONECUT 1 (HNF6) were also up-regulated (Fig. 2). These data indicate that hepatocyte-related genes are considerably up-regulated in AT-MSC-Hepa, human hepatocytes and human liver when compared with undifferentiated AT-MSCs. We also focused on genes that are responsible for basic functions of hepatocytes (Table 1). Cytochrome P450 genes, including CYP2A6, CYP2C8 and CYP3A4, and ABC transporter genes such as MDR1 (multi-drug resistance), which play an important role in drug metabolism and detoxification, are highly

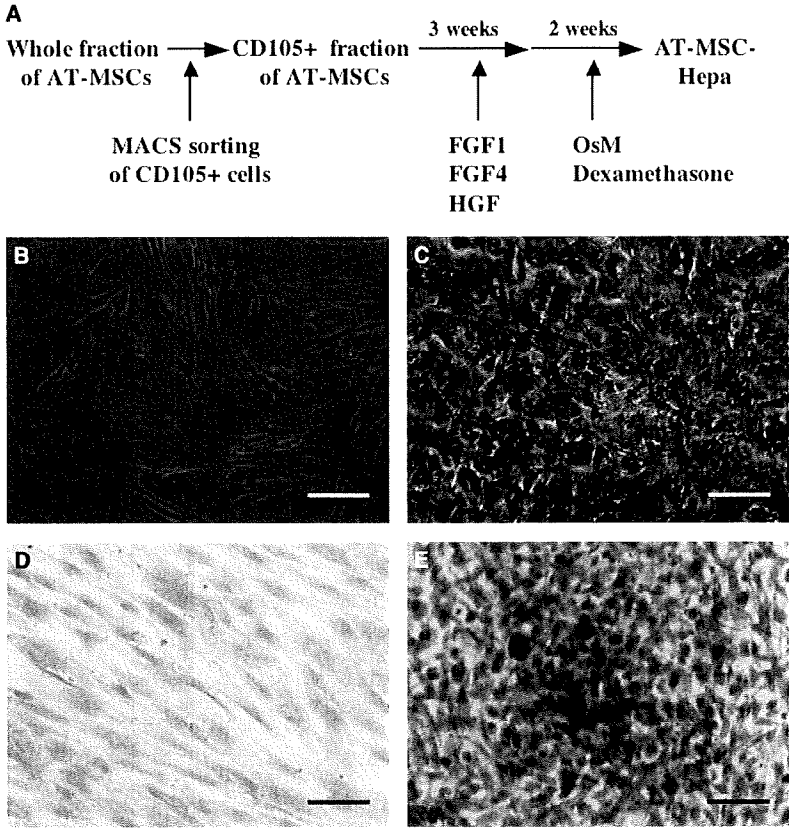

Fig. 1. Hepatic differentiation of human AT-MSC. (A) Schematic illustration outlining the differentiation protocol. The $CD105^+$ fraction was isolated from whole fraction of AT-MSCs of using CD105-coupled magnetic microbeads. These cells were treated with HGF (150 $ng \cdot mL^{-1}$), FGF1 (300 $ng \cdot mL^{-1}$) and FGF4 (25 $ng \cdot mL^{-1}$) for 3 weeks, and with oncostatin M (30 $ng \cdot mL^{-1}$) and dexamethasone (2×10^5 $mol \cdot L^{-1}$) for the next 2 weeks. (B,C) Phase-contrast micrographs of undifferentiated $CD105^+$ AT-MSCs and AT-MSC-Hepa, respectively. (D,E) Periodic acid-Schiff staining of undifferentiated $CD105^+$ AT-MSCs and AT-MSC-Hepa, respectively. Scale bars = 50 μm.

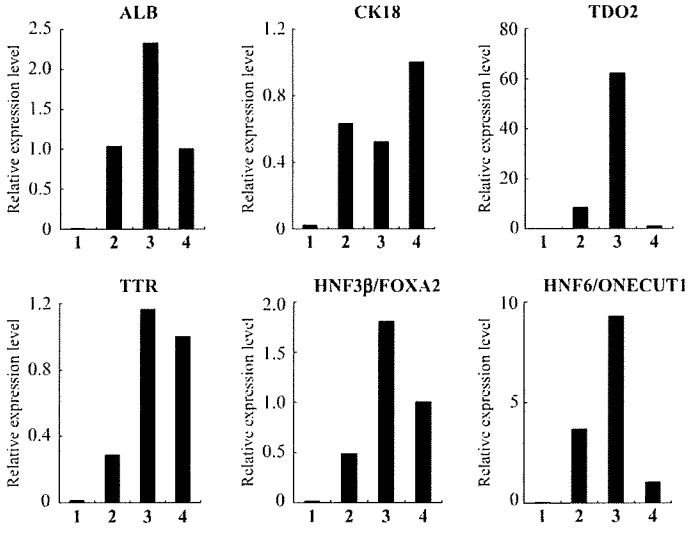

Fig. 2. Comparison of the expression pattern of selected liver-specific genes by microarray analysis. Expression patterns of ALB, transthyretin, TDO2, CK18, HNF3β/FOXA2 and HNF6/ONECUT1: lane 1, undifferentiated AT-MSCs; lane 2, human liver; lane 3, AT-MSC-Hepa; lane 4, human primary hepatocytes. The expression level of human hepatocytes was set to 1.0.

induced by hepatic differentiation treatment of AT-MSCs. A number of genes encoding a blood coagulation factor, a complement component and a component of the extracellular matrix, which are involved in hepatocyte maintenance and functionality, were also up-regulated. Genes that were down-regulated genes after hepatic differentiation of AT-MSCs include cyclin B2 and E2F1 (supplementary Table S2), which are responsible for cell-cycle control. Together, the results suggest that HIFC treatment induced

Table 1. Liver function genes that were up-regulated in AT-MSC-Hepa.

Accession number	Description	Relative expression levels			
		AT-MSCs	AT-MSC-derived hepatocytes	Human liver	Human hepatocytes
CYP450					
AF355802	CYP3A5 mRNA, allele CYP3A5, exon 5B and partial CDS, alternatively spliced	0.02	1.75	8.71	1.00
NM_031226	cytochrome P450, family 19, subfamily A, polypeptide 1, transcript variant 2	0.05	5.51	0.13	1.00
NM_000762	cytochrome P450, family 2, subfamily A, polypeptide 6	0.05	0.61	493.31	1.00
NM_000770	cytochrome P450, family 2, subfamily C, polypeptide 8, transcript variant Hp1-1	0.06	6.23	348.38	1.00
NM_000775	cytochrome P450, family 2, subfamily J, polypeptide 2	0.01	0.32	2.01	1.00
NM_000500	cytochrome P450, family 21, subfamily A, polypeptide 2	0.18	3.22	3.96	1.00
NM_057157	cytochrome P450, family 26, subfamily A, polypeptide 1, transcript variant 2	0.02	0.42	1.85	1.00
NM_017460	cytochrome P450, family 3, subfamily A, polypeptide 4	0.01	1.72	16.75	1.00
NM_000765	cytochrome P450, family 3, subfamily A, polypeptide 7	0.01	10.04	5.38	1.00
NM_016593	cytochrome P450, family 39, subfamily A, polypeptide 1	0.02	0.96	4.27	1.00
NM_000779	cytochrome P450, family 4, subfamily B, polypeptide 1	0.65	21.02	1.20	1.00
NM_021187	cytochrome P450, family 4, subfamily F, polypeptide 11	0.02	0.25	3.92	1.00
NM_023944	cytochrome P450, family 4, subfamily F, polypeptide 12	0.01	0.16	1.77	1.00
NM_000896	cytochrome P450, family 4, subfamily F, polypeptide 3	0.04	1.25	10.45	1.00
NM_004820	cytochrome P450, family 7, subfamily B, polypeptide 1	0.09	1.55	4.67	1.00
NM_004391	cytochrome P450, family 8, subfamily B, polypeptide 1	0.01	0.63	24.42	1.00
ABC transporter					
NM_173076	ATP-binding cassette, sub-family A, member 12, transcript variant 1	0.56	6.28	1.37	1.00
NM_001089	ATP-binding cassette, sub-family A, member 3	0.01	0.33	0.13	1.00
NM_080284	ATP-binding cassette, sub-family A, member 6, transcript variant 1	0.39	4.61	16.06	1.00
NM_000927	ATP-binding cassette, sub-family B, member 1	0.01	0.70	0.76	1.00
NM_003742	ATP-binding cassette, sub-family B, member 11	0.05	1.98	13.24	1.00
NM_018850	ATP-binding cassette, sub-family B, member 4, transcript variant C	0.01	0.55	6.34	1.00
NM_033151	ATP-binding cassette, sub-family C, member 11, transcript variant 2	0.03	0.31	9.81	1.00
NM_000392	ATP-binding cassette, sub-family C, member 2	0.02	0.29	0.79	1.00
NM_020038	ATP-binding cassette, sub-family C, member 3, transcript variant MRP3B	0.02	0.35	0.81	1.00
NM_022436	ATP-binding cassette, sub-family G, member 5	0.02	0.80	2.59	1.00
Coagulation					
NM_000506	coagulation factor II	0.01	0.35	2.83	1.00
NM_000133	coagulation factor IX	0.01	2.49	98.68	1.00
NM_000130	coagulation factor V	0.02	3.52	19.54	1.00
NM_000131	coagulation factor VII, transcript variant 1	0.02	1.05	12.16	1.00
NM_000504	coagulation factor X	0.07	0.82	6.36	1.00
NM_000128	coagulation factor XI, transcript variant 1	0.02	2.48	35.85	1.00
NM_000505	coagulation factor XII	0.02	0.25	9.25	1.00
NM_001994	coagulation factor XIII, B polypeptide	0.05	4.36	34.09	1.00
NM_000508	Fibrinogen α chain, transcript variant α-E	0.01	19.55	138.80	1.00
NM_005141	Fibrinogen β chain	0.01	4.41	27.34	1.00
NM_000509	Fibrinogen γ chain, transcript variant γ-A	0.01	5.72	17.75	1.00
NM_201553	Fibrinogen-like 1, transcript variant 4	0.01	1.40	6.20	1.00
Complement component					
NM_015991	complement component 1, q subcomponent, α polypeptide	0.16	8.98	116.43	1.00

Table 1. (Continued).

Accession number	Description	Relative expression levels			
		AT-MSCs	AT-MSC-derived hepatocytes	Human liver	Human hepatocytes
NM_000491	complement component 1, q subcomponent, β polypeptide	0.03	12.04	112.80	1.00
NM_000063	complement component 2	0.03	0.61	5.62	1.00
NM_000064	complement component 3	0.01	1.94	6.09	1.00
NM_000715	complement component 4 binding protein, α	0.01	1.23	23.89	1.00
NM_000716	complement component 4 binding protein, β, transcript variant 1	0.01	0.25	3.24	1.00
NM_000592	complement component 4B	0.02	1.81	11.11	1.00
NM_001735	complement component 5	0.40	24.82	119.11	1.00
NM_000065	complement component 6	0.01	9.27	104.33	1.00
NM_000562	complement component 8, α polypeptide	0.03	0.71	61.32	1.00
NM_000066	complement component 8, β polypeptide	0.01	1.07	39.23	1.00
NM_001737	complement component 9	0.01	1.61	158.48	1.00
NM_000186	complement factor H, transcript variant 1	0.99	19.22	61.60	1.00
NM_002113	complement factor H-related 1	0.66	11.11	45.93	1.00
NM_005666	complement factor H-related 2	0.02	2.55	180.30	1.00
NM_021023	complement factor H-related 3	0.51	8.25	23.81	1.00
NM_006684	complement factor H-related 4	0.03	2.61	119.37	1.00
NM_030787	complement factor H-related 5	0.55	9.08	924.13	1.00
Lipid metabolism					
NM_000039	apolipoprotein A-I	0.01	0.21	3.76	1.00
NM_001643	apolipoprotein A-II	0.01	0.36	2.27	1.00
NM_000384	apolipoprotein B	0.01	6.26	29.22	1.00
NM_001645	apolipoprotein C-I	0.01	0.42	3.37	1.00
NM_000483	apolipoprotein C-II	0.01	0.55	0.67	1.00
NM_001647	apolipoprotein D	0.66	808.87	1.20	1.00
NM_000041	apolipoprotein E	0.01	1.62	5.08	1.00
NM_001638	apolipoprotein F	0.07	1.11	361.43	1.00
NM_000042	apolipoprotein H	0.01	0.30	4.60	1.00
NM_001443	fatty acid binding protein 1, liver	0.01	2.17	9.56	1.00
NM_000236	lipase, hepatic	0.01	1.05	1.57	1.00
NM_139248	lipase, member H	0.01	0.66	0.02	1.00
NM_000237	lipoprotein lipase	0.58	314.81	17.32	1.00
NM_018557	Low-density lipoprotein-related protein 1B	0.71	41.48	1.40	1.00
NM_004525	Low-density lipoprotein-related protein 2	0.66	23.96	9.80	1.00
NM_015900	phospholipase A1 member A	0.20	7.46	23.23	1.00
NM_000300	phospholipase A2, group IIA	0.11	1.66	266.80	1.00
NM_005084	phospholipase A2, group VII	0.55	24.55	72.21	1.00
NM_032562	phospholipase A2, group XIIB	0.01	0.87	2.57	1.00
NM_014996	Phospholipase C-like 3	0.52	14.14	1.25	1.00
Matrix					
NM_033380	Collagen, type IV, α5, transcript variant 2	6.07	68.67	17.94	1.00
NM_033641	Collagen, type IV, α6, transcript variant B	0.58	15.10	1.38	1.00
NM_030582	Collagen, type XVIII, α1, transcript variant 1	0.08	1.68	2.80	1.00
NM_198129	Laminin, α3, transcript variant 1	0.02	0.44	0.10	1.00
NM_005560	Laminin, α5	0.08	0.81	0.37	1.00
NM_005562	Laminin, γ2, transcript variant 1	0.05	0.52	0.01	1.00
NM_000638	Vitronectin	0.04	1.00	7.18	1.00

differentiation of AT-MSCs into cells with a gene expression profile typical of mature hepatocytes.

To validate the results of the microarray analysis, we selected several genes expressed in AT-MSCs and analyzed them using real-time RT-PCR. The expression level of up-regulated genes such as albumin and TDO2 was confirmed by this method, and this analysis indicated the accuracy of the results regarding

transcriptional regulation obtained in the microarray experiments (data not shown).

Unsupervised clustering analysis of AT-MSC-Hepa

Unsupervised hierarchical cluster analysis was performed by sorting of 1639 altered genes (Fig. 3A). This analysis of microarray data revealed a striking similarity of gene clusters among AT-MSC-Hepa, primary hepatocytes and human liver. This indicates that AT-MSC-Hepa are similar to human hepatocytes with respect to the gene expression pattern. Figure 3B shows a cluster of genes that are up-regulated in AT-MSC-Hepa, primary hepatocytes and human liver, and includes a number of liver function genes; for example, complement components, coagulation factors, apolipoprotein. Other clusters of genes up-regulated in AT-MSC-Hepa are also hepatocyte-specific (data not shown). In addition, to assess robustness, bootstrap re-sampling was performed with 100 iterations. A cluster of AT-MSCs (lane 1) was a truly robust cluster, with a bootstrap re-sampling value of approximately 100%, suggesting that the gene expression pattern in AT-MSCs is significantly different from that in AT-MSC-Hepa.

Taken together, hierarchical clustering analysis of the differentiated AT-MSCs indicates a very similar gene expression pattern to that of primary hepatocytes and a different pattern from that of AT-MSCs.

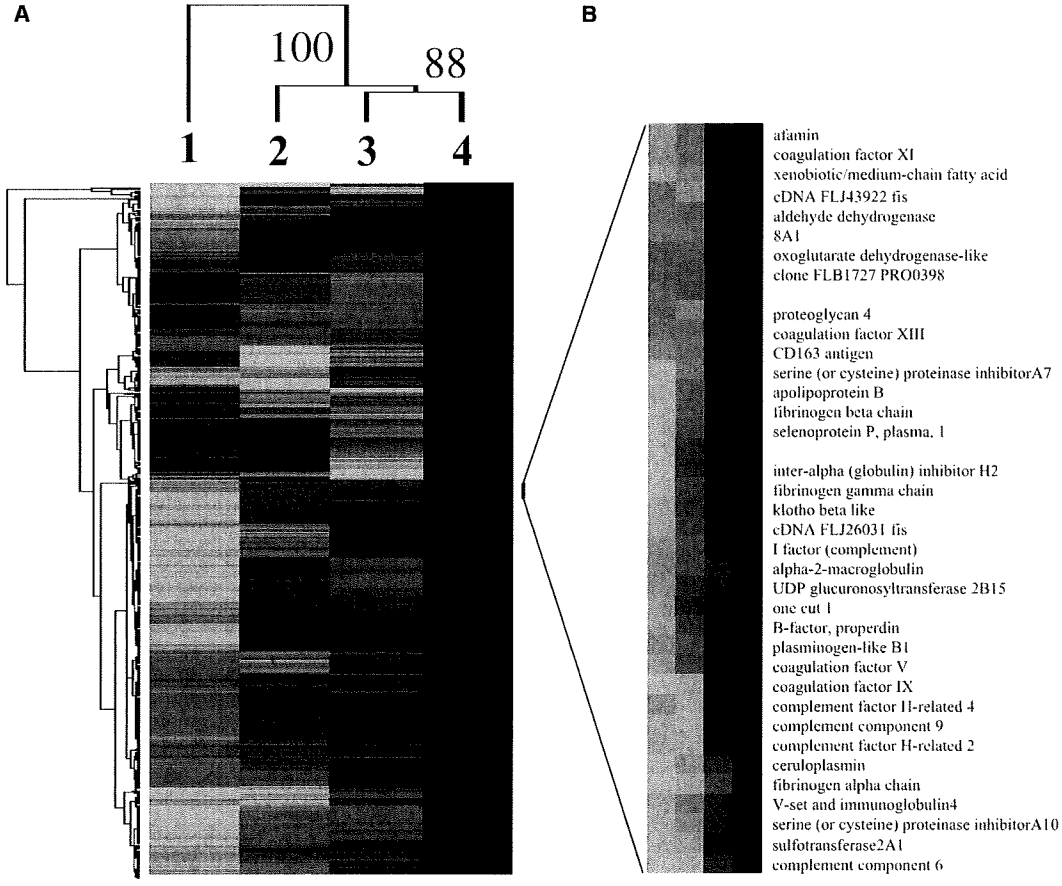

Fig. 3. Unsupervised hierarchical analysis of 1639 gene expression profiles. (A) Data were subjected to hierarchical cluster analysis using an Euclidean distance calculation based on Ward method. Lane 1, undifferentiated AT-MSCs; lane 2, human liver; lane 3, AT-MSC-Hepa; lane 4, human primary hepatocytes. Samples are linked by the dendrogram above to show the similarity of their gene expression patterns. The expression profile of each gene is represented in the respective rows. Genes are linked by the dendrogram on the left to show the similarity in their expression patterns. Bootstrap re-sampling was performed with 100 iterations. Red, black and green represent high, middle and low expression levels, respectively. The expression level of each gene in the human primary hepatocyte sample was set to 1.0. (B) Representative gene cluster chosen to show that hepatic function-related genes are up-regulated in human liver, AT-MSC-Hepa and human primary hepatocytes.

Gene ontology (GO) classification of AT-MSC-Hepa

Using a database, the microarray analysis data were integrated to identify the gene ontology (GO) biological processes for the up- and down-regulated genes. This analysis indicated that GO groups were highly significant for up- and down-regulated genes compared with the parent population (Table 2). The probabilities of observing such a high number of genes in these categories by chance were extremely small, ranging from 8.9×10^{-24} to 6.4×10^{-3}. In up-regulated genes, most of these GO groups, such as those relating to blood coagulation, lipid metabolism and fibrinolysis, are relevant to hepatocyte function, suggesting that AT-MSCs undergo precise hepatic induction. Therefore, the enrichment of liver function genes in AT-MSC-Hepa was statistically significant. In contrast, for example, the gene categories relating to cell cycle and organelle localization were significantly down-regulated in AT-MSC-Hepa. This indicates that the cell proliferation rate of AT-MSCs decreases during hepatic differentiation. Thus, the results of GO analysis suggest that AT-MSC-Hepa have numerous hepatocyte functions compared with undifferentiated AT-MSCs.

Gene signaling pathways in AT-MSC-Hepa

Elucidating the gene network pathway functioning in AT-MSC-Hepa is very important to reveal the processes of hepatic induction and maintenance of the hepatocyte function. Recently, we developed a new microarray system, ConPath ('concise pathway', conpath.dna-chip.co.jp/), to analyze biological pathways. This microarray system also enables us to re-evaluate data obtained using the Agilent microarray. The probes on the ConPath Chip represent genes that are found in the pathways contributed to the GENMAPP database (see Experimental procedures). These biological pathways are established pathways contributed by the biological community and serve as a good reference to evaluate microarray data in the context of biological functions and pathways. Expression ratios of AT-MSC-Hepa, undifferentiated AT-MSCs and human liver relative to human primary hepatocytes, obtained using the ConPath microarray, were further

Table 2. Significance of gene ontology category appearance for the up- and down-regulated genes in AT-MSC-Hepa.

GO term	Cluster frequency[a]	Percentage	Sample frequency of use[b]	Percentage	*P* value[c]
Up-regulated genes					
Inflammatory response	64/739	8.66	227/12 441	1.82	8.88E-24
Complement activation	22/739	2.98	33/12 441	0.27	1.02E-16
Innate immune response	24/739	3.25	59/12 441	0.47	9.70E-12
Blood coagulation	25/739	3.38	78/12 441	0.63	1.58E-09
Adaptive immune response	17/739	2.30	43/12 441	0.35	1.46E-07
Response to chemical stimulus	49/739	6.63	326/12 441	2.62	1.83E-06
Circulation	22/739	2.98	99/12 441	0.80	7.16E-05
Hormone metabolism	15/739	2.03	48/12 441	0.39	7.64E-05
Lipid metabolism	64/739	8.66	539/12 441	4.33	8.74E-05
Steroid metabolism	26/739	3.52	135/12 441	1.09	0.0001
Cytolysis	8/739	1.08	15/12 441	0.12	0.00083
Response to xenobiotic stimulus	10/739	1.35	25/12 441	0.20	0.00093
Carboxylic acid metabolism	48/739	6.50	392/12 441	3.15	0.00167
Nitrogen compound metabolism	42/739	5.68	330/12 441	2.65	0.00287
Fibrinolysis	6/739	0.81	9/12 441	0.07	0.00389
Down-regulated genes					
Cell division	31/215	14.42	178/12 441	1.43	9.28E-20
Cell cycle	53/215	24.65	675/12 441	5.43	1.97E-18
Chromosome segregation	12/215	5.58	43/12 441	0.35	3.61E-09
Organelle localization	5/215	2.33	13/12 441	0.10	0.00122
Cytoskeleton organization and biogenesis	19/215	8.84	346/12 441	2.78	0.0064

[a] Of the genes analyzed, the GO biological process is known for 739 up-regulated genes and 215 down-regulated genes. Others are unknown. [b] Of the genes in the mother population, the GO biological process is known for 12 441. Others are unknown. [c] The significance of the appearance of the GO term (biological process) in the up-regulated and down-regulated genes was calculated as a *P* value by the software GO Term Finder.

analyzed using GENMAPP software version 2.1 and visualized using ConPath Navigator, a tool that enables viewing and searching of results obtained by GENMAPP analysis (unpublished results; GENMAPP details available at http://www.genmapp.org). Biological pathways relating to liver function selected from the pathways in this microarray are listed in Table 3. The number of genes in each pathway that showed elevated expression (fold change > 1, log ratio) were compared with the total number of genes in each pathway. The number of genes up-regulated in AT-MSC-Hepa, when compared with human hepatocytes, in each pathway was similar to that of human liver, indicating that biological pathways related to liver function are equivalent between AT-MSC-Hepa and human liver (Table 3). Noticeably, of the 20 genes in the blood clotting cascade that are included on the chip, a total of 14 and 15 genes were elevated in AT-MSC-Hepa and human liver, respectively (Table 3 and supplementary Fig. S1). Furthermore, in the classical complementary activation pathway (Fig. 4), the expression pattern of AT-MSC-Hepa (Fig. 4b) was closer to that of human liver (Fig. 4c) than to that of undifferentiated AT-MSC (Fig. 4a). Likewise, the fatty acid omega oxidation and steroid biosynthesis pathways were clearly up-regulated in AT-MSC-Hepa, compared to undifferentiated AT-MSCs (supplementary Figs S1 and S3). Therefore, this analysis provided evidence that the majority of liver functions are detected in AT-MSC-Hepa, as well as in human hepatocytes and human liver.

Table 3. Comparison of the number of genes up-regulated[a] in AT-MSC-Hepa and human liver for each liver-related signal pathway.

Signal pathway	AT-MSC-Hepa	Whole liver	Number of genes included on ConPath chip
Blood clotting cascade	14	15	20
Complement activation, classical pathway	12	16	17
Eicosanoid synthesis	14	12	19
Fatty acid omega oxidation	6	11	15
Glucocorticoid and mineralcorticoid metabolism	4	6	9
Glutathione metabolism	11	9	20
Glycogen metabolism	7	12	36
Steroid biosynthesis	4	6	9
Synthesis and degradation of ketone bodies	3	4	5
Urea cycle and metabolism nof amino groups	8	9	20

[a] The expression level of the gene is higher (fold change > 1) compared with the expression level in human hepatocytes (reference sample).

Mesenchymal-to-epithelial transition in AT-MSC-Hepa

Although AT-MSCs do indeed differentiate into hepatocyte-like cells *in vitro*, concern remains about transdifferentiation and its molecular mechanism. To address the molecular basis of the transition of AT-MSCs to a hepatic phenotype, we focused especially on genes relating to the mesenchymal–epithelial transition (MET), the process that mesodermal cells (AT-MSCs) undergo during differentiation to hepatocytes, which have epithelial-like morphology. Microarray data indicated that the expression levels of Twist [17] and Snail [18], which are regulators of the epithelial–mesenchymal transition (EMT), were down-regulated during the differentiation process (Table 4). Furthermore, epithelial markers such as E-cadherin and α-catenin were up-regulated in AT-MSC-Hepa. In contrast, the expression of mesenchymal markers such as N-cadherin and vimentin was down-regulated (Table 4). During hepatic differentiation, morphological modification from a fibroblastic shape in AT-MSC to an epithelial cell-like morphology in AT-MSC-Hepa was observed. These findings support the notion that MET occurs in the process of hepatic differentiation from AT-MSCs. Although further investigations are required to elucidate the molecular mechanism of transdifferentiation of AT-MSCs into hepatic cells, the findings presented here suggest that MET might be a pivotal factor in determining stem cell transdifferentiation.

Discussion

AT-MSCs may be good candidates as stem cells for cell transplantation and tissue engineering in regenerative medicine, as a large number of AT-MSCs can be obtained easily with minimal invasiveness by liposuction. Recently, we have produced mature hepatocytes by direct differentiation of AT-MSCs, without the necessity for co-culture with fetal or adult hepatocytes. We have shown that our system induced transplantable cells with morphological and functional characteristics of hepatocytes [16]. Other groups have also provided evidence of hepatic differentiation from human AT-MSC [13,14]. None of the reports, however, provided a comprehensive analysis of the process underlying the differentiation of AT-MSCs into hepatocytes. In this report, we clearly demonstrated the utility of microarray analysis in proving the hepatic differentiation of AT-MSCs. Moreover, analysis of GO groups indicated that many of the 1639 up- or down-regulated genes belonged to GO categories relevant to hepatic

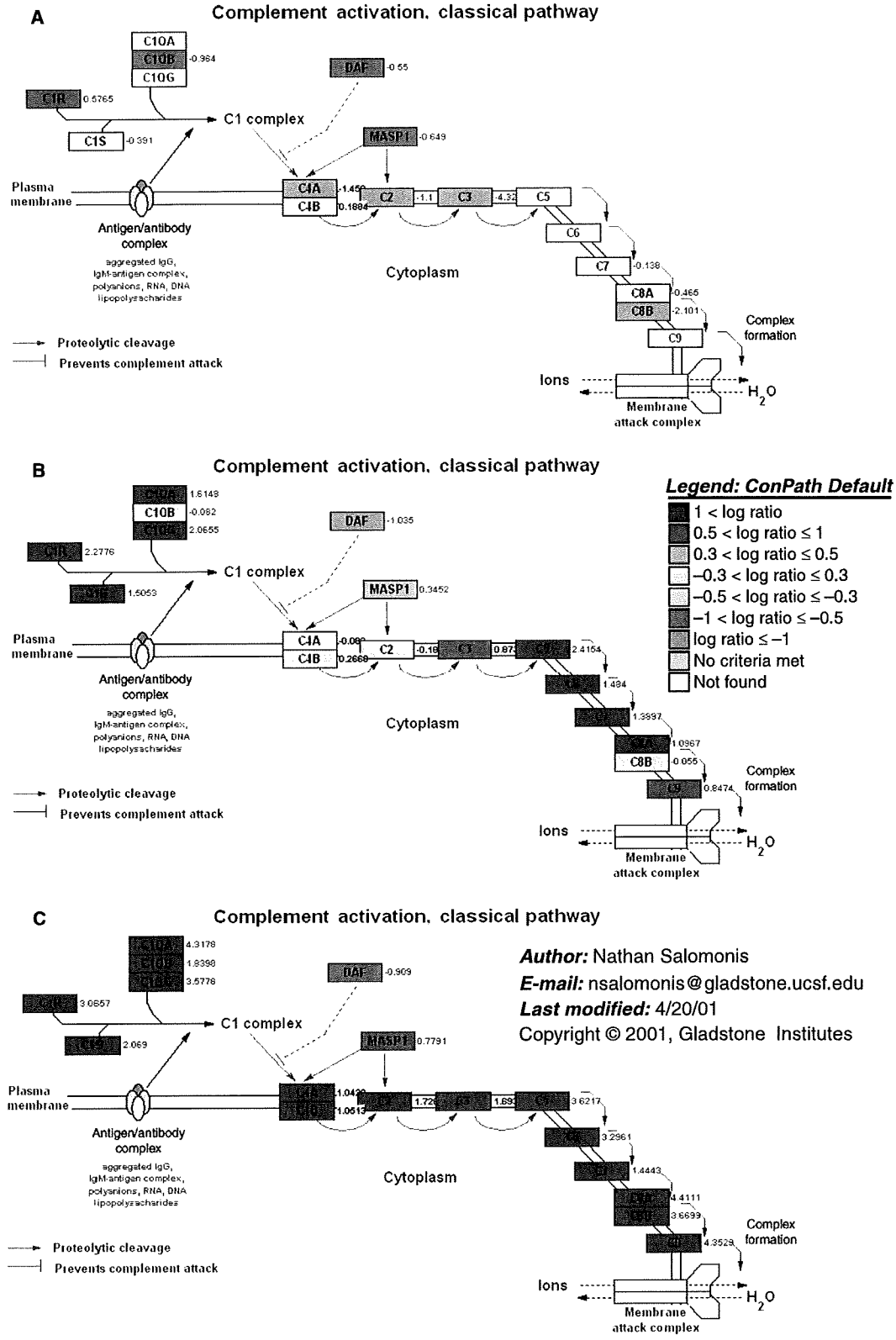
A
Complement activation, classical pathway
C1QA
C1QB
C1QG
-0.964
C1R
0.5765
C1S
-0.391
C1 complex
DAF
-0.55
MASP1
-0.649
Plasma membrane
C4A
C4B
0.1884
C2
-1.1
C3
-4.32
C5
C6
C7
-0.138
C8A
C8B
-0.465
-2.101
C9
Complex formation
Antigen/antibody complex
aggregated IgG, IgM-antigen complex, polyanions, RNA, DNA lipopolysacharides
Cytoplasm
Ions
H_2O
Membrane attack complex
Proteolytic cleavage
Prevents complement attack
B
Complement activation, classical pathway
1.6148
C1QB
-0.082
2.0655
2.2776
1.5053
C1 complex
DAF
-1.035
MASP1
0.3452
Plasma membrane
C4A
-0.088
C4B
0.2668
C2
-0.16
0.87
2.4164
1.484
1.3997
1.0967
C8B
-0.055
0.8474
Complex formation
Antigen/antibody complex
aggregated IgG, IgM-antigen complex, polyanions, RNA, DNA lipopolysacharides
Cytoplasm
Ions
H_2O
Membrane attack complex
Proteolytic cleavage
Prevents complement attack
Legend: ConPath Default
1 < log ratio
0.5 < log ratio ≤ 1
0.3 < log ratio ≤ 0.5
−0.3 < log ratio ≤ 0.3
−0.5 < log ratio ≤ −0.3
−1 < log ratio ≤ −0.5
log ratio ≤ −1
No criteria met
Not found
C
Complement activation, classical pathway
4.3178
1.8398
3.5778
3.0857
2.069
C1 complex
DAF
-0.909
MASP1
0.7791
Plasma membrane
1.0429
1.0613
1.72
1.69
3.6217
3.2961
1.4443
4.4111
3.6699
4.3529
Complex formation
Antigen/antibody complex
aggregated IgG, IgM-antigen complex, polyanions, RNA, DNA lipopolysacharides
Cytoplasm
Ions
H_2O
Membrane attack complex
Proteolytic cleavage
Prevents complement attack
Author: Nathan Salomonis
E-mail: nsalomonis@gladstone.ucsf.edu
Last modified: 4/20/01
Copyright © 2001, Gladstone Institutes

function, including steroid and lipid metabolism. In addition, gene signaling pathway analysis has identified gene signals that are remarkably activated in AT-MSC-Hepa, and these signals are also up-regulated in whole liver. Therefore, the microarray analysis provides a potentially valuable resource for determination of the key molecules involved in hepatocyte differentiation and function. These integrative perspectives on the gene expression profile might be useful for revealing the control of plasticity of AT-MSCs that give rise to hepatocytes.

Just prior to birth and shortly thereafter, a large number of liver metabolic enzymes are induced. After birth, the liver acquires additional metabolism functions and becomes fully mature [19]. Some cytochrome P450 genes are also expressed after birth and play an important role in drug metabolism. Using microarray analysis, a number of cytochrome P450 genes were clearly identified as up-regulated in AT-MSC-Hepa. Additional studies have indicated that several cytochrome P450 proteins were expressed in AT-MSC-Hepa (unpublished results). Activities of CYP1A2, CYP2B6, CYP2C19, CYP2D6 and CYP3A were clearly detected, and these activities were approximately ≥ 10-fold lower than those of primary hepatocytes. In particular, the enzyme activity of CYP2C9 in AT-MSC-Hepa was remarkably high compared to that in primary hepatocytes.

CYP3A4 is a major cytochrome P450 gene that is expressed in the human liver [20], and its product is involved in the metabolism of 45–60% of the drugs metabolized by cytochrome P450 proteins [21,22]. Our data indicate that the amount of CYP3A4 expressed in AT-MSC-Hepa is approximately 170 times higher than that in undifferentiated AT-MSCs. Additionally, microarray analysis indicated that the expression level of the ABC transporter gene MDR-1, which is implicated in expelling various drugs from cells, was also remarkably higher than that in undifferentiated AT-MSCs [23]. CYP3A4 and MDR-1 are two major factors that modulate exposure to a large range of xenobiotics [24]. Clinical studies of biotransformation of newly developed drugs in humans are subject to several constraints, including ethics, cost and time. Considerable emphasis has therefore been placed on the development of *in vitro* test systems. Although primary human hepatocytes are the best source of cells for such systems, their use for this purpose is limited by donor shortage and the difficulties involved in adequate propagation and long-term maintenance of normal human hepatocytes in culture. Thus, our cells might be suitable as an alternative for the validation of newly developed drugs, because they express CYP3A4 and MDR-1 at levels comparable to those in primary human hepatocytes.

Expression of liver-selective transcription factors, such as HNFs, CCAAT/enhancer-binding proteins and GATA-binding proteins, is essential for the induction of liver development and its progression. These transcription factors exhibit temporal- and site-specific expression patterns during organogenesis, with a distinct narrow time interval of transcription initiation [25], and regulate transactivation of several endoderm- and hepatocyte-specific factors, including transthyretin, albumin and tyrosine aminotransferase [26,27]. It has been reported that HNF3β/FOXA2 plays an important role in endoderm specification and subsequent hepatocyte differentiation *in vivo* and *in vitro* [28,29]. In this study, induction of HNF3β/FOXA2 expression was clearly seen in AT-MSC-Hepa by microarray analysis. Furthermore, our data demonstrated that expression of other hepatic transcription factors, including HNF3α/FOXA1, GATA4, HNF6/ONECUT1 and HNF1, were ≥ 10-fold up-regulated in AT-MSC-Hepa compared with undifferentiated AT-MSCs. These results suggest that transcription factor networks are precisely regulated in the hepatic differentiation system, and that the AT-MSCs differentiate into mature hepatocytes.

Mesencyhmal-to-epithelial transition is the reverse of the epithelial–mesenchymal transition (EMT) that is a crucial event in cancer progression and embryonic development [30]. We found evidence of transdifferentiation by MET in the process of hepatic differentiation of AT-MSCs. No previous report has demonstrated evidence of transdifferentiation of committed adult stem cells. In the case of our study, transdifferentiation, in which AT-MSCs, which have a mesodermal phenotype, are converted to hepatocytes, with an epithelial cell-like phenotype, might be caused by MET [31,32]. As shown in our previous immunocytochemical study and shown by the results of this microarray analysis, AT-MSCs express a mesenchymal marker, vimentin. Expression of the epithelial marker E-cadherin was remarkably up-regulated (81-fold) in AT-MSC-Hepa, compared with undifferentiated

Fig. 4. Complementary activation, classical pathway. The expression levels of genes of AT-MSC (A), AT-MSC-Hepa (B) and human liver (C), when compared to human hepatocytes, are shown on this illustration of the classical complementary activation pathway created by Nathan Salomonis using GENMAPP version 2.1. Most of the expression levels of genes in this pathway were lower (green, see color legend) or undetected (no coloring) in AT-MSC (A), but were higher (red) in AT-MSC-Hepa (B) and human liver (C).

Table 4. Expression levels of EMT-related genes in AT-MSCs and AT-MSC-Hepa.

	AT-MSCs	AT-MSC-Hepa	Ratio
EMT regulators			
Twist1	16.74	10.36	0.62
Twist2	345.76	205.26	0.59
Snail1	7.25	2.77	0.38
Snail2	11.71	5.18	0.44
Epithelial markers			
E-cadherin	0.01	0.81	81.04
α-catenin	0.46	0.63	1.35
Mesenchymal markers			
N-cadherin	0.99	0.69	0.70
Vimentin	2.11	1.68	0.79

AT-MSCs. Furthermore, microarray-based integrated analysis of methylation by isoschizomers (MIAMI) [33] was utilized for genome-wide profiling of the DNA methylation status of AT-MSCs and AT-MSC-Hepa. Preliminary data show that the promoter region of 39 genes was hypermethylated and that of eight genes was hypomethylated in AT-MSC-Hepa. It is noteworthy that the promoter region of the Twist was hypermethylated in AT-MSC-Hepa, indicating that expression of the Twist gene was suppressed by epigenetical modification (unpublished results). These data support the evidence for transdifferentiation by MET in AT-MSC-Hepa. Although the relationship between the altered DNA methylation status for the other genes identified and hepatic differentiation is not yet understood, these genome-wide methylation findings will also help to clarify the mechanism of hepatic differentiation from AT-MSCs.

This report provides evidence that the transcriptome and signal pathways of AT-MSC-Hepa are similar to those of human primary hepatocytes and that hepatic differentiation has occurred through MET. Human fetal hepatocytes are the current standard model system for the study of mature hepatocytes. Drawbacks include the limited amount of cells that can be obtained from an individual, a limited life span, and an inability to withstand freeze/thaw procedures. Therefore, our system will provide a valuable tool, in addition to primary hepatocytes, for study of the molecular basis of the regenerative and developmental processes of hepatic cells *in vitro*.

Experimental procedures

Hepatic differentiation by the HIFC method

Isolation and culture of AT-MSCs were as described previously [16]. The AT-MSCs used for microarray analysis were obtained from a gastric cancer patient (55 years old, male, height 164 cm, weight 67.2 kg) undergoing gastrectomy at the International Medical Center of Japan, Tokyo. The ethics committee of the hospital approved this study, and informed consent was obtained from the patient. The $CD105^+$ fraction was isolated from AT-MSCs using CD105-coupled magnetic microbeads (Miltenyi Biotec, Bergisch Galdbach, Germany) [16]. Briefly, hepatic induction of AT-MSCs was performed over a period of 3 weeks by culturing in hepatocyte culture medium containing transferrin (5 $\mu g \cdot mL^{-1}$), hydrocortisone-21-hemisuccinate (10^{-6} M), BSA (0.5 $mg \cdot mL^{-1}$), ascorbic acid (2 mM), epidermal growth factor (20 $ng \cdot mL^{-1}$), insulin (5 $\mu g \cdot mL^{-1}$), gentamycin (50 $\mu g \cdot mL^{-1}$) (Cambrex, Walkersville, MD, USA) and dexamethasone (10^{-8} M), and supplemented with HIFC containing HGF (150 $ng \cdot mL^{-1}$), FGF1 (300 $ng \cdot mL^{-1}$) and FGF4 (25 $ng \cdot mL^{-1}$) (PeproTech EC, London, UK). For the next 2 weeks, the cells were treated with oncostatin M (30 $ng \cdot mL^{-1}$) and dexamethasone (2×10^{-5} $mol \cdot L^{-1}$) and then cultured in hepatocyte culture medium alone for 5 weeks.

Isolation of total RNA

Total RNA was extracted from undifferentiated AT-MSCs, AT-MSC-Hepa, human primary hepatocytes and human liver using ISOGEN solution (Nippon Gene, Tokyo, Japan) according to the manufacturer's protocol, and then treated with deoxyribonuclease (DNase I, amplification grade; TaKaRa, Kyoto, Japan).

Microarray analysis and data mining (Aligent array)

A one-color microarray-based gene expression analysis system (Agilent Technologies, Tokyo, Japan) containing 41 000 clones was used, according to the manufacturer's instructions. Total RNA was extracted from undifferentiated AT-MSCs, AT-MSC-Hepa, human primary hepatocytes and human liver. The RNA sample of human primary hepatocytes was used as the total RNA reference. The process of hybridization and washing was performed using a Gene Expression Wash Pack (Agilent Technologies) and acetonitrile (Sigma, Tokyo, Japan). A DNA microarray scanner (Agilent Technologies) was used for array scanning. To ensure data reliability, weak signal spots were removed according to the manufacturer's criteria. This resulted in a data matrix of 25 721 genes with no missing data.

Hierarchical undifferentiated clustering analysis

Genes that showed a ≥ 10-fold increase or decrease in the expression level in AT-MSC-Hepa compared to undifferentiated AT-MSCs were designated as up- or down-regulated genes, respectively. A hierarchical cluster was produced from

the up- and down-regulated gene data using an Euclidean distance calculation based on the Ward method calculation by GENMATHS software (Applied Maths, Austin, TX, USA).

Gene ontology analysis

Gene ontology categories were assigned to genes based on the ACEGENE microarray database (DNA Chip Research Inc. and Hitachi Software Co., Yokohama, Japan). The significance of GO term appearance in the up- and down-regulated genes (compared with all 12 441 annotated genes) was calculated using the software GO Term Finder adapted to the ACEGENE microarray (http://db.yeastgenome.org/cgi-bin/SGD/GO/goTermFinder). Cut-off points were set at 0.01 [34].

RNA target preparation and hybridization procedures for microarray experiment (ConPath method)

RNA was amplified using a MessageAmp™ II-biotin-enhanced single-round amplified RNA amplification kit (Ambion, Austin, TX, USA). Briefly, 1 μg total RNA for each sample was transcribed into double-stranded T7 RNA polymerase promoter-tagged cDNA, then amplified into single-stranded biotin-labeled cRNA using T7 polymerase. Aliquots (3 μg) of cRNA were fragmented at 94 °C for 15 min and hybridized onto a ConPath™ chip (DNA Chip Research Inc., GEO ID GPL5437) in the presence of formamide (final concentration 10% v/v) at 37 °C for 16 h. The chip was washed at room temperature for 5 min in 0.1× SSC, 0.1% SDS, followed by another 5 min wash in 0.05× SSC, 0.1% SDS at 43 °C. Finally, the chip was rinsed in 0.05× SSC before drying by low-speed centrifugation. For staining, the chip was immersed in an NaCl/P_i solution containing 10 $\mu g \cdot mL^{-1}$ of streptavidin/R-phycoerythrin conjugate (Invitrogen, Carlsbad, CA, USA), Tween-20 (0.05% v/v) and BSA (2 $mg \cdot mL^{-1}$) for 30 min. A wash in NaCl/P_i for 5 min at room temperature was performed to remove any additional stain, followed by another wash in a similar buffer, separately prepared, for 30 s. The chip was rinsed in 0.05× SSC at room temperature before drying by low-speed centrifugation.

Measurement and data analysis (ConPath method)

The chip was scanned using an Agilent DNA microarray scanner at a resolution of 10 μm (photo-multiplier tube: 80). Intensity values of each feature of the scanned image were quantified using Feature EXTRACTION software (version 9.1, Agilent Technologies), which performs background subtractions. Features that were flagged according to the software ALGORITHM or that were below background value were excluded from further analysis. Normalization was performed using GENESPRING Gx. version 7.3.1 (per chip: normalization to 50th percentile; per gene: normalization to control reference sample) (Agilent Technologies). Expression ratios were calculated for features that which were present in both reference and tested samples. GENMAPP version 2.1 [35,36] (http://www.genmapp.org) analysis was performed using gene database Hs-Std_20060526.gdb.

Acknowledgements

This work was supported in part by a grant-in-aid from the Third-Term Comprehensive 10-Year Strategy for Cancer Control, health science research grants for Research on the Human Genome and Regenerative Medicine from the Ministry of Health, Labor and Welfare of Japan, a grant from the Japanese Health Sciences Foundation, and a grant for research fellowships from the Japanese Society for the Promotion of Science for Young Scientists. We thank Dr Gary Quinn, Dr Fumitaka Takeshita, Dr Shinobu Ueda, Ms Ayako Inoue, Ms Maho Kodama, and Ms Nachi Namatame for their excellent technical assistance, and Research & Development projects for supporting regional small and medium enterprises.

References

1 Friedenstein AJ, Latzinik NW, Grosheva AG & Gorskaya UF (1982) Marrow microenvironment transfer by heterotopic transplantation of freshly isolated and cultured cells in porous sponges. *Exp Hematol* **10**, 217–227.
2 Zuk PA, Zhu M, Ashjian P, De Ugarte DA, Huang JI, Mizuno H, Alfonso ZC, Fraser JK, Benhaim P & Hedrick MH (2002) Human adipose tissue is a source of multipotent stem cells. *Mol Biol Cell* **13**, 4279–4295.
3 Zuk PA, Zhu M, Mizuno H, Huang J, Futrell JW, Katz AJ, Benhaim P, Lorenz HP & Hedrick MH (2001) Multilineage cells from human adipose tissue: implications for cell-based therapies. *Tissue Eng* **7**, 211–228.
4 Shih DT, Lee DC, Chen SC, Tsai RY, Huang CT, Tsai CC, Shen EY & Chiu WT (2005) Isolation and characterization of neurogenic mesenchymal stem cells in human scalp tissue. *Stem Cells* **23**, 1012–1020.
5 In't Anker PS, Scherjon SA, Kleijburg-van der Keur C, de Groot-Swings GM, Claas FH, Fibbe WE & Kanhai HH (2004) Isolation of mesenchymal stem cells of fetal or maternal origin from human placenta. *Stem Cells* **22**, 1338–1345.
6 Bieback K, Kern S, Kluter H & Eichler H (2004) Critical parameters for the isolation of mesenchymal stem cells from umbilical cord blood. *Stem Cells* **22**, 625–634.
7 Campagnoli C, Roberts IA, Kumar S, Bennett PR, Bellantuono I & Fisk NM (2001) Identification of

mesenchymal stem/progenitor cells in human first-trimester fetal blood, liver, and bone marrow. *Blood* **98**, 2396–2402.
8 Pittenger MF, Mackay AM, Beck SC, Jaiswal RK, Douglas R, Mosca JD, Moorman MA, Simonetti DW, Craig S & Marshak DR (1999) Multilineage potential of adult human mesenchymal stem cells. *Science* **284**, 143–147.
9 Ferrari G, Cusella-De Angelis G, Coletta M, Paolucci E, Stornaiuolo A, Cossu G & Mavilio F (1998) Muscle regeneration by bone marrow-derived myogenic progenitors. *Science* **279**, 1528–1530.
10 Sanchez-Ramos J, Song S, Cardozo-Pelaez F, Hazzi C, Stedeford T, Willing A, Freeman TB, Saporta S, Janssen W, Patel N *et al.* (2000) Adult bone marrow stromal cells differentiate into neural cells in vitro. *Exp Neurol* **164**, 247–256.
11 Sato Y, Araki H, Kato J, Nakamura K, Kawano Y, Kobune M, Sato T, Miyanishi K, Takayama T, Takahashi M *et al.* (2005) Human mesenchymal stem cells xenografted directly to rat liver are differentiated into human hepatocytes without fusion. *Blood* **106**, 756–763.
12 Hong SH, Gang EJ, Jeong JA, Ahn C, Hwang SH, Yang IH, Park HK, Han H & Kim H (2005) In vitro differentiation of human umbilical cord blood-derived mesenchymal stem cells into hepatocyte-like cells. *Biochem Biophys Res Commun* **330**, 1153–1161.
13 Seo MJ, Suh SY, Bae YC & Jung JS (2005) Differentiation of human adipose stromal cells into hepatic lineage in vitro and in vivo. *Biochem Biophys Res Commun* **328**, 258–264.
14 Talens-Visconti R, Bonora A, Jover R, Mirabet V, Carbonell F, Castell JV & Gomez-Lechon MJ (2007) Human mesenchymal stem cells from adipose tissue: differentiation into hepatic lineage. *Toxicol In Vitro* **21**, 324–329.
15 Teratani T, Yamamoto H, Aoyagi K, Sasaki H, Asari A, Quinn G, Terada M & Ochiya T (2005) Direct hepatic fate specification from mouse embryonic stem cells. *Hepatology* **41**, 836–846.
16 Banas A, Teratani T, Yamamoto Y, Tokuhara M, Takeshita F, Quinn G, Okochi H & Ochiya T (2007) Adipose tissue-derived mesenchymal stem cells as a source of human hepatocytes. *Hepatology* **46**, 219–228.
17 Yang J, Mani SA, Donaher JL, Ramaswamy S, Itzykson RA, Come C, Savagner P, Gitelman I, Richardson A & Weinberg RA (2004) Twist, a master regulator of morphogenesis, plays an essential role in tumor metastasis. *Cell* **117**, 927–939.
18 Peinado H, Olmeda D & Cano A (2007) Snail, Zeb and bHLH factors in tumour progression: an alliance against the epithelial phenotype? *Nat Rev Cancer* **7**, 415–428.
19 Kamiya A, Kojima N, Kinoshita T, Sakai Y & Miyaijma A (2002) Maturation of fetal hepatocytes in vitro by extracellular matrices and oncostatin M: induction of tryptophan oxygenase. *Hepatology* **35**, 1351–1359.
20 Watkins PB (1994) Noninvasive tests of CYP3A enzymes. *Pharmacogenetics* **4**, 171–184.
21 Bertz RJ & Granneman GR (1997) Use of in vitro and in vivo data to estimate the likelihood of metabolic pharmacokinetic interactions. *Clin Pharmacokinet* **32**, 210–258.
22 Evans WE & Relling MV (1999) Pharmacogenomics: translating functional genomics into rational therapeutics. *Science* **286**, 487–491.
23 Ambudkar SV, Kimchi-Sarfaty C, Sauna ZE & Gottesman MM (2003) P-glycoprotein: from genomics to mechanism. *Oncogene* **22**, 7468–7485.
24 Cavaco I, Gil JP, Gil-Berglund E & Ribeiro V (2003) CYP3A4 and MDR1 alleles in a Portuguese population. *Clin Chem Lab Med* **41**, 1345–1350.
25 Costa RH, Kalinichenko VV, Holterman AX & Wang X (2003) Transcription factors in liver development, differentiation, and regeneration. *Hepatology* **38**, 1331–1347.
26 Duncan SA, Navas MA, Dufort D, Rossant J & Stoffel M (1998) Regulation of a transcription factor network required for differentiation and metabolism. *Science* **281**, 692–695.
27 Bossard P & Zaret KS (1998) GATA transcription factors as potentiators of gut endoderm differentiation. *Development* **125**, 4909–4917.
28 Yamamoto Y, Teratani T, Yamamoto H, Quinn G, Murata S, Ikeda R, Kinoshita K, Matsubara K, Kato T & Ochiya T (2005) Recapitulation of in vivo gene expression during hepatic differentiation from murine embryonic stem cells. *Hepatology* **42**, 558–567.
29 Lee CS, Friedman JR, Fulmer JT & Kaestner KH (2005) The initiation of liver development is dependent on Foxa transcription factors. *Nature* **435**, 944–947.
30 Kang Y & Massague J (2004) Epithelial–mesenchymal transitions: twist in development and metastasis. *Cell* **118**, 277–279.
31 Zipori D (2004) Mesenchymal stem cells: harnessing cell plasticity to tissue and organ repair. *Blood Cells Mol Dis* **33**, 211–215.
32 Nakaya Y, Kuroda S, Katagiri YT, Kaibuchi K & Takahashi Y (2004) Mesenchymal–epithelial transition during somatic segmentation is regulated by differential roles of Cdc42 and Racl. *Dev Cell* **7**, 425–438.
33 Hatada I, Fukasawa M, Kimura M, Morita S, Yamada K, Yoshikawa T, Yamanaka S, Endo C, Sakurada A, Sato M *et al.* (2006) Genome-wide profiling of promoter methylation in human. *Oncogene* **25**, 3059–3064.

34 Haverty PM, Hansen U & Weng Z (2004) Computational inference of transcriptional regulatory networks from expression profiling and transcription factor binding site identification. *Nucleic Acids Res* **32**, 179–188.
35 Doniger SW, Salomonis N, Dahlquist KD, Vranizan K, Lawlor SC & Conklin BR (2003) MAPPFinder: using Gene Ontology and GenMAPP to create a global gene-expression profile from microarray data. *Genome Biol* **4**, R7.
36 Dahlquist KD, Salomonis N, Vranizan K, Lawlor SC & Conklin BR (2002) GenMAPP, a new tool for viewing and analyzing microarray data on biological pathways. *Nat Genet* **31**, 19–20.

Supplementary material

The following supplementary material is available for this article online:

Fig. S1. The classical pathway of complementary activation.
Fig. S2. The fatty acid omega oxidation pathway.
Fig. S3. The steroid biosynthesis pathway.
Table S1. Genes that were up-regulated AT-MSC-Hepa.
Table S2. Genes that were down-regulated in AT-MSC-Hepa.

This material is available as part of the online article from http://www.blackwell-synergy.com

Please note: Blackwell Publishing are not responsible for the content or functionality of any supplementary materials supplied by the authors. Any queries (other than missing material) should be directed to the corresponding author for the article.

doi:10.1111/j.1440-1746.2008.05496.x

HEPATOLOGY

Rapid hepatic fate specification of adipose-derived stem cells and their therapeutic potential for liver failure

Agnieszka Banas,* Takumi Teratani,* Yusuke Yamamoto,*,† Makoto Tokuhara,‡ Fumitaka Takeshita,* Mitsuhiko Osaki,* Takashi Kato,† Hitoshi Okochi‡ and Takahiro Ochiya*

*Section for Studies on Metastasis, National Cancer Center Research Institute, Chuo-ku, †Department of Biology, School of Education, Waseda University, Shinjuku-ku, and ‡Department of Surgery, International Medical Center of Japan, Shinjuku, Tokyo, Japan

Key words
adipose, differentiation, hepatocyte, liver regeneration, mesenchymal stem cell.

Accepted for publication 13 April 2008.

Correspondence
Dr Takahiro Ochiya, Section for Studies on Metastasis, National Cancer Center Research Institute, 1-1, Tsukiji 5-chome, Chuo-ku, Tokyo 104-0045, Japan. Email: tochiya@ncc.go.jp

Abstract

Background and Aim: Multipotential mesenchymal stem cells (MSC), present in many organs and tissues, represent an attractive tool for the establishment of a successful stem cell-based therapy in the field of regeneration medicine. Adipose tissue mesenchymal stem cells (AT-MSC), known as adipose-derived stem cells (ASC) are especially attractive in the context of future clinical applications because of their high accessibility and minimal invasiveness during the procedure to obtain them. The goal of the present study was to induce human ASC into functional hepatocytes *in vitro* within a very short period of time and to check their therapeutic potential *in vivo*.

Methods: *In vitro* generated ASC-derived hepatocytes were checked for hepatocyte-specific markers and functions. Afterwards, they were transplanted into nude mice with liver injury. Twenty-four hours after transplantation, biochemical parameters were evaluated in blood serum.

Results: We have shown here that ASC can be differentiated into hepatocytes within 13 days and can reach the functional properties of primary human hepatocytes. After transplantation into mice with acute liver failure, ASC-derived hepatocytes can restore such liver functions as ammonia and purine metabolism. Markers of liver injury, alanine aminotransferase, aspartate aminotransferase, as well as ammonia, were decreased after ASC-derived hepatocyte transplantation.

Conclusions: Our data highlight the properties of ASC as having a special affinity for hepatocyte differentiation *in vitro* and liver regeneration *in vivo*. Thus, ASC may be a superior choice for the establishment of a therapy for injured liver.

Introduction

The liver is exposed to many factors such as drugs, xenobiotics and viruses, which cause chronic hepatitis and liver cirrhosis. In most cases these lead to hepatocellular carcinoma and finally to organ failure, where there is chronic inflammation, fibrosis and no longer any regeneration ability.[1]

At present, liver transplantation is the only effective treatment for severe liver injuries. However, because of organ rejection and lack of donors, alternative strategies are urgently needed.

Human primary hepatocytes are commercially available; however, maintaining them in *in vitro* culture is very difficult, if not nearly impossible. After a few days of *in vitro* culturing they lose their functions. Additionally, their usage does not solve the problem of rejection. These factors limit their experimental applications and exclude their clinical usage.

In the last few years, extrahepatic cell populations with the potential to impact liver diseases have been discovered. The potential candidate stem cells for therapy of an injured liver are mesenchymal stem cells (MSC), which can be obtained from different sources such as bone marrow (BM),[2] umbilical cord blood (UCB),[3] amniotic fluid (AF),[4] scalp tissue,[5] placenta,[6] or adipose tissue (AT)[7,8] of the human body. These cells reveal a multipotentiality and semi-infinite proliferation ability. The hepatogenic differentiation capacity of MSC has been confirmed in many independent studies on BM-MSC,[9–14] UCB-MSC,[15–16] and adipose-derived stem cells (ASC).[17–19] The possibility for their future application in the therapy of liver diseases is very promising. MSC can easily be obtained from a patient's own tissues, isolated *ex vivo*, expanded, differentiated toward hepatocytes, and transplanted back into the patient in the form of either undifferentiated MSC or MSC-derived hepatocytes. Such a possibility sidesteps the limits regarding ethical issues and immunocompatibility problems. Importantly, MSC represent an advantageous cell type for allogenic transplantation as well, because they are immuno-privileged with low major histocompatibility complex (MHC) I (histocompatibility

Journal of Gastroenterology and Hepatology **24** (2009) 70–77